

# Dual Polarized Antenna with Wide Beamwidth Utilizing TM01 Mode for X-Band Applications

Hayam Mohy<sup>1</sup>, Anwer S. Abd El-Hameed<sup>2</sup>, Member, IEEE, Hany A. Atallah<sup>1, □</sup>, and Adel B. Abdel-Rahman<sup>1,3</sup>



**Abstract** This paper presents a triple-port dual-polarized antenna designed for X-band applications with a wide beamwidth. The antenna utilizes 50  $\Omega$  probe feeding structure, resulting in a small size of  $20 \times 20$  mm<sup>2</sup>. The proposed antenna is developed for X-band applications, operating at 10.7 GHz with a bandwidth of 200 MHz. The structure comprises two stacked substrates with electrical properties (2.2, and 4.5 permittivities, 1.5 mm height). The top layer features a rectangular patch with two ports for exciting orthogonal polarizations, while the middle layer includes a circular patch serving as a ground plane for the rectangular patch. The excitation of TM01 mode in the circular patch generates a conical radiation pattern, and the antenna exhibits an overlapping bandwidth from 10.3 GHz to 10.9 GHz. The peak gains, illustrated over the frequency range, reach 5.2 dBi for the circular patch and 7 dBi for the rectangular patch. Fabrication and measurements of the antenna demonstrate good agreement between experimental and simulation results.

**Keywords:** Antenna, beamwidth, dual polarized, patch, triple-port, X-band.

## 1 Introduction

Microstrip patch antennas stand out as a favored antenna design, primarily owing to their compact dimensions, straightforward fabrication, and seamless integration with monolithic microwave integrated circuits [1-5]. The rectangular and circular patches of

these antennas allow for the excitation of various radiated modes, each with distinct radiation characteristics [6], [7]. The coaxial probe feed serves as an effective means to generate specific modes, such as TM01 or TM02, resulting in broadside pattern radiation, as exemplified in prior works [8], [9]. This design offers a notable advantage in its reduced size compared to a quarter-wavelength monopole antenna, making it suitable for indoor applications and various mobile communication systems. To enhance impedance matching across dual bands, a stacking technique was implemented specifically for the circular patch [10]. The adoption of the TM02 mode results in a conical radiation pattern. An alternative approach, presented in [11], involves configuring a ring cluster of microstrip-patch antennas to achieve conical radiation.

The polarization diversity technique is widely employed in contemporary wireless communication systems and base stations, surpassing spatial diversity in popularity due to its cost-effectiveness in installation and performance enhancement in channel conditions. Unlike spatial diversity, polarization diversity requires only a single-element installation [12].

In existing literature [13-31], dual-polarization antennas have been designed by employing orthogonal feeding structures to excite the antenna [13], [14]. Achieving adequate isolation between the two ports of the dual-polarization antenna is crucial for optimal performance. Aperture-coupling, a popular feeding technique, is utilized to mitigate strong coupling between the horizontal and vertical components of the antenna [15]. In a specific instance [16], an L-shaped probe feed was employed to achieve high isolation between the dual-polarization antennas.

In [17, 18], a dual-polarization antenna featuring a conical radiation pattern was successfully developed. The horizontal polarization was attributed to the formation of a stable horizontal current loop within the cross-slot, while vertical polarization was achieved

Received: 8 January 2024/ Accepted: 5 February 2024

□Corresponding Author Hany A. Atallah,  
h.atallah@eng.svu.edu.eg

1. Electrical Engineering Department, Faculty of Engineering,  
South Valley University, Qena 83523, Egypt

2. Electronics Research Institute (ERI), Giza, Egypt.

3. EJUST, Electronics and Communications Engineering,  
Alexandria 21934, Egypt.

through a long monopole. Another innovative design, presented in [19], introduced a dual-polarized slot "cusp" antenna capable of dual omnidirectional patterns by exciting either its slot-line mode or coplanar mode. However, these designs fell short of achieving dual conical patterns.

Reconfigurable antennas have recently garnered significant interest due to the simplicity of the design process [20]. Various reconfigurable structures have been developed specifically for polarization-diversity purposes [21]. In [22], a quadric-polarization-diversity patch antenna was achieved by manipulating the radiation pattern through a control circuit. The suggested design offered right-handed and left-handed circularly polarized (CP) as well as orthogonal linearly polarized (LP) patterns. While capable of exciting four different polarizations, these designs were limited to broadside radiation patterns. Another noteworthy development is described in [23], where the radiation pattern was reconfigured from conical to a broadside shape. It is important to note that modifying the shape of the radiation pattern can offer an additional degree of freedom for portable devices. However, the introduction of controlling circuits and DC biasing in reconfigurable antennas, while facilitating ease of design and control over the radiation pattern, can lead to violations of antenna symmetry and compromises in the quality of the radiation pattern.

This paper presents a dual-polarization antenna for X-band applications with a wide beamwidth radiation pattern. The design achieves broad beamwidth by combining the broadside radiation pattern from the rectangular patch's fundamental mode and the conical radiation pattern from the TM<sub>01</sub> mode of the circular patch. Dual stacked substrates with permittivities of 4.5 and 2.2 enhance antenna efficiency. A probe feeding technique is employed for a compact profile ( $20 \times 20 \text{ mm}^2$ ). The design incorporates a dual-polarized rectangular patch on the top layer and a circular patch on the second layer as a ground plane. Conical radiation is achieved by exciting the TM<sub>01</sub> mode through a shorting connection between the circular patch and the ground, facilitated by a circular copper sheet. The proposed antenna demonstrates a wide bandwidth from 10.3 GHz to 10.9 GHz.

## 2 Antenna Design

### 2.1 Design Geometry

The geometry of the proposed antenna is depicted in Fig. 1. The structure comprises two substrates, with the upper substrate being Rogers RT5880 with permittivity and thickness denoted as  $h_1 = 1.5 \text{ mm}$ , and the lower substrate being FR4 with permittivity 4.5 and thickness  $h_2 = 1.5 \text{ mm}$ , while the copper thickness is  $t = 0.035 \text{ mm}$ . A shorted circular annular ring patch is positioned on the bottom substrate, and a square patch is affixed to the top substrate. The circular patch is fed using a feeding probe. To excite the TM<sub>01</sub> mode (conical pattern), shorting pins are strategically inserted into the circular patch [24]. For ease of antenna fabrication, the shorting pins are replaced by a copper sheet, achievable with copper clad. The coaxial probe is located at a distance  $X$  from the patch edge. The inner and outer dimensions of the annular ring govern the resonance frequency.

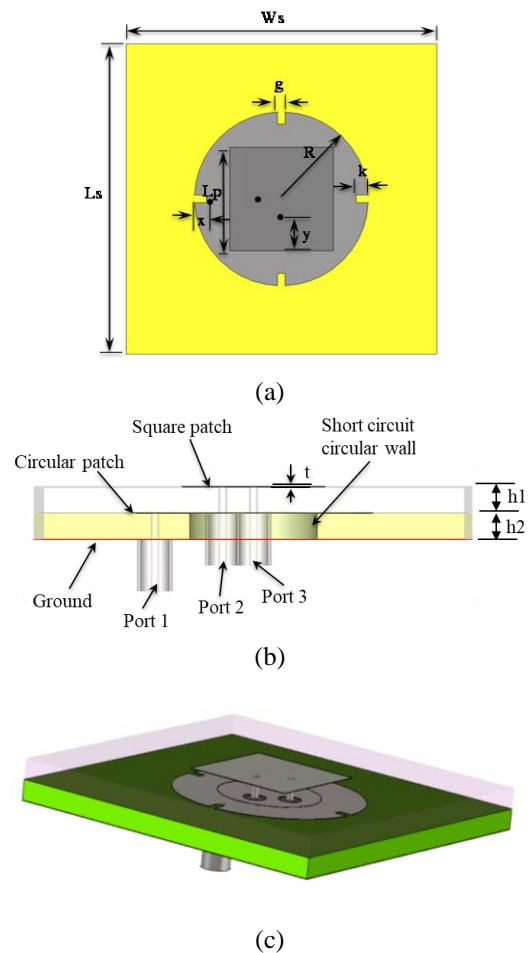


Fig.1 The geometry of the proposed antenna, showcasing (a) a top view, (b) a cross-section, and (c) a 3D perspective.

Dual polarizations at the fundamental frequency are generated in the square patch by utilizing two orthogonal probe feeding structures. The dimensions of the

rectangular patch are computed to align with the frequency of the TM01 mode of the shorted annular ring patch antenna. The annular ring's higher-order modes offer the advantage of a conical radiation pattern, while the rectangular patch contributes to a broadside radiation pattern. Combining both features in a single antenna enables the attainment of a wide beamwidth. The optimized dimensions for the entire structure are provided in Table 1.

Table 1 Optimized dimensions for the proposed design in mm.

Ws	Ls	R	Lp	h1	h2	x	y	k	g
25	25	7	8.3	1.5	1.5	1.1	2.4	1	0.6

## 2.2 Principle of operation

The suggested configuration consists of two superimposed patches, with the top one being rectangular and the lower one adopting an annular ring shape. The annular ring is formed by a circular disc incorporating a short-circuit wall with a radius of 3.75 mm. By treating the short-circuited annular ring patch as a cavity confined by electric walls at the upper and lower edges and assuming the presence of only the TM mode propagating within this cavity, the resonance frequencies can be determined using equation (1). It is assumed that the metal thickness has negligible impact on the field distribution, given that the metal thickness is significantly smaller than the wavelength.

$$f_{mn} = \frac{k_{mn}}{n\pi a \cdot \sqrt{\mu_0 \cdot \epsilon}} = \frac{k_{mn} \cdot c}{2\pi a \cdot \sqrt{\epsilon_r}} \quad (1)$$

Where,  $mn$  are the TM mode numbers,  $\epsilon$  is substrate permittivity,  $\epsilon_r$  is the substrate relative permittivity,  $\mu_0$  is the free space permeability  $a$  is the annular ring outer radius, and  $K_{mn}$  are the roots of the following characteristic equation (2) [25].

$$J'_m(k_{mn})N_m(k_{mn}c) - J_m(k_{mn})N'_m(k_{mn}c) = 0 \quad (2)$$

In this context,  $J_m(x)$  and  $N_m(x)$  represent the first and second kind  $m$ th order Bessel functions, respectively, where  $c$  is the ratio  $b/a$  in Equation (2). This equation is primarily derived from imposing boundary conditions within the annular ring cavity, where the inner edge is characterized by an electric wall and the outer edge by a magnetic wall. The  $n$ th index for

the corresponding TM01 mode is consistently set to 1, while the  $m$ th index can vary from 0 to 4. Consequently, the mode is determined by the  $m$ th index, and it's important to note that the zero mode corresponds to the lowest frequency. Conversely, the dual-port rectangular patch can achieve dual polarization by orthogonal excitation.

## 3 Results and Discussions

In this section, which focuses on the results of the proposed antenna, the outcomes of the conducted analysis and the overall performance evaluation are comprehensively presented and discussed.

### 3.1 Parametric Analysis

In this section, the focus is on the parametric analysis, specifically examining the impact of variations in the rectangular patch length ( $L_p$ ) and circular patch radius ( $R$ ) on the antenna's resonant frequency. Fig. 2(a) and Fig. 2(b) visually illustrate this impact. Through systematic adjustments of  $L_p$  and  $R$ , the study aims to elucidate their roles in shaping the resonant characteristics of the antenna. Valuable insights into the optimization and tuning process are provided, contributing to a clearer understanding of how the antenna responds to variations in  $L_p$  and  $R$ . This parametric analysis is crucial in refining the design for optimal operational efficiency in X-band applications.

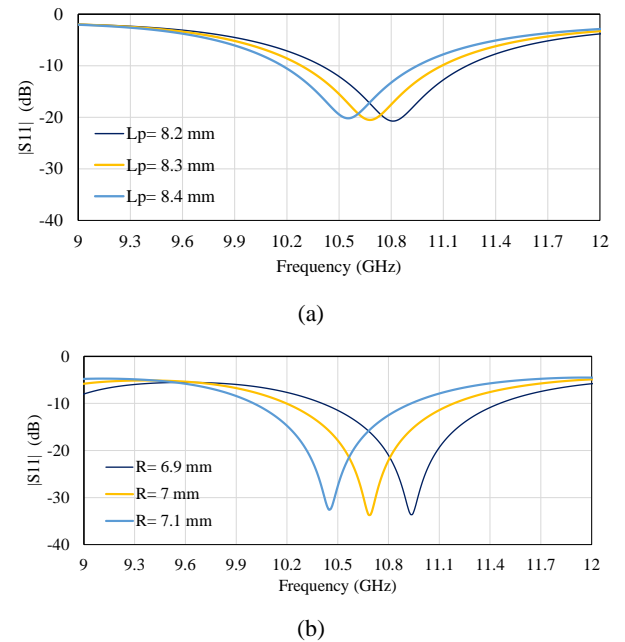


Fig. 2 A parametric analysis on the primary parameters of the radiating patches, showcasing variations in (a)  $L_p$  and (b)  $R$ .

### 3.1 Current Distributions

The current distribution in the described triple-port dual-polarized antenna is characterized by the interplay of its key design elements. In the top layer, a rectangular patch with two ports facilitates the excitation of orthogonal polarizations. The current distribution across this layer is influenced by the input signals and the geometry of the rectangular patch as shown in Fig. 3 (a) and (b). The currents flowing through the second and third ports are perpendicular to one another. Simultaneously, the middle layer features a circular patch functioning as the ground plane for the rectangular patch. The excitation of the TM<sub>01</sub> mode in the circular patch induces a specific current distribution shown in Fig.3 (c), generating a conical radiation pattern. This distribution is a result of the electromagnetic interactions within the structure and is pivotal in shaping the overall performance of the antenna. The interconnection of current flows across the stacked substrates and patches contributes to the achievement of a wide beamwidth and an overlapping bandwidth from 10.3 GHz to 10.9 GHz.

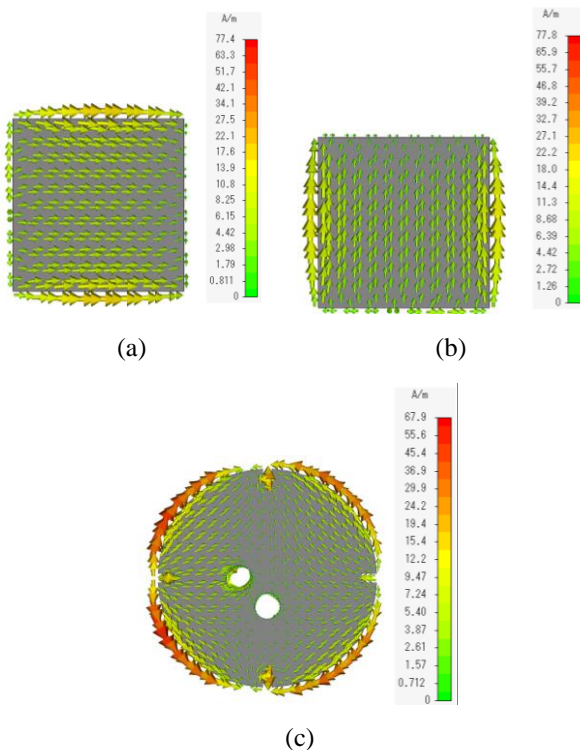
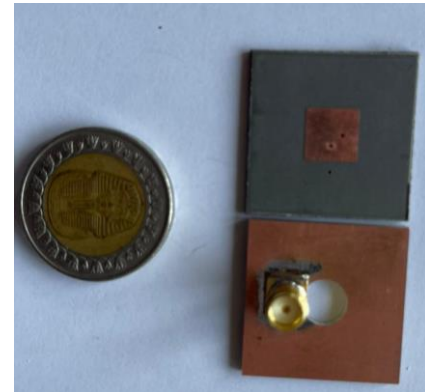


Fig.3 Current distribution scenarios when (a) the antenna is excited at Port 2, (b) the antenna is excited from Port 3, and (c) the antenna is excited from Port 1.

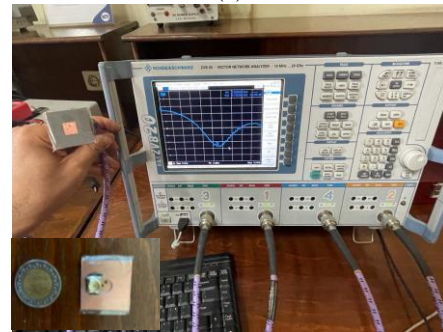
## 4 Fabrication and Measurements

A dual-polarized antenna with a wide beamwidth

was designed, fabricated, and tested, as depicted in the photograph presented in Fig. 4. The design and fabrication involved the utilization of Rogers RT5880 and FR4 substrates. Copper clad was employed to facilitate the shortening between the circular patch and the ground. The reflection coefficient of the antenna was measured using a vector network analyzer (ROHDE & SCHWARZ ZVA 67), while its radiation pattern is presented as a simulation.



(a)



(b)

Fig.4 Fabrication and measurements, showcasing (a) The fabricated prototype. (b) The measurement setup of S-parameters.

In Fig. 5, a comparison is presented between the simulated and measured reflection coefficient and transmission coefficient results for the fabricated antenna. The measured impedance bandwidth, below -10 dB, for the proposed antenna covers a range of 10.3 GHz to 10.9 GHz for the rectangular patch and extends from 10.3 GHz to 11.3 GHz for the circular disc. Fig. 6 illustrates the simulated radiation patterns at 10.7 GHz, revealing a wide beamwidth. In Fig. 7, the graph illustrates the simulated peak gain with frequency, reaching 5.2 dBi for the circular patch and 7 dBi for the rectangular patch. Fig. 8 depicts the radiation efficiency, reaching 89%, and 98% at the center frequency for circular and rectangular patches respectively. Table 2 summarizes key parameters of different antenna designs,

showcasing their frequencies, volumes, bandwidths, gains, and port configurations. Our stacked patch antenna, situated within recent investigations, demonstrates an advantageous blend of frequency, compact dimensions, bandwidth, and gain, underscoring its competitive position in current antenna research. Despite [27] achieving the widest bandwidth, its gain remains relatively low.

Table 2 Comparison with Prior Studies.

Ref.	Ant. type	Freq. (GHz)	Volume ( $\lambda^3$ )	BW (%)	Gain	ports
[26]	horn	10.00	2.87×2.87×1.5	7	7.3	1
[27]	Slot	5.62	1.12×1.12×0.09	25.6	6	1
[28]	Patch	2.61	0.87×0.87×0.03	5.7	2.7	1
This Work	Satcked Patches	10.70	1.5 × 1.5×0.11	5.7	7	2

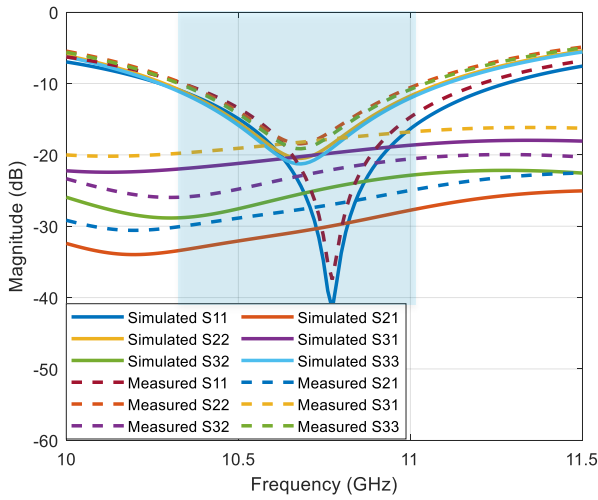


Fig.5 Measured and simulated S-parameters versus frequency.

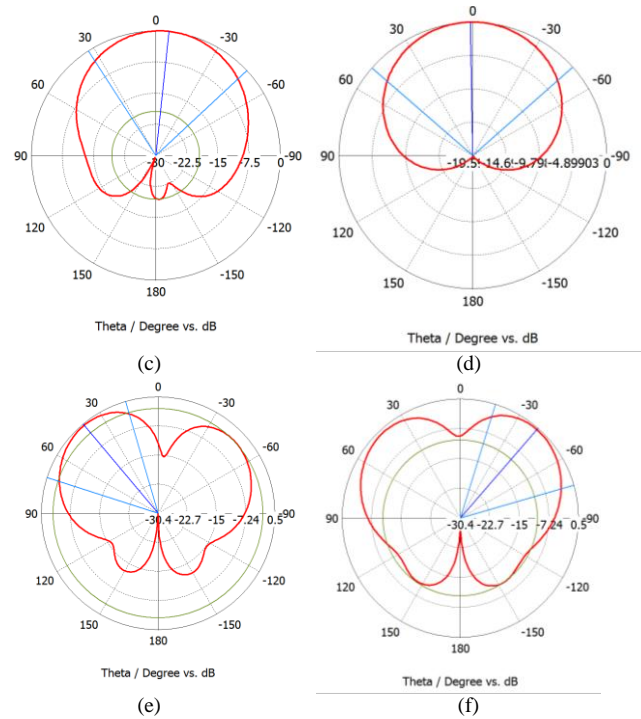
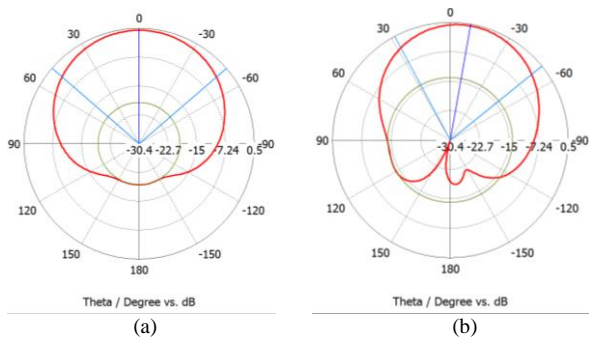


Fig.6 The radiation patterns of the proposed antenna at 10.7 GHz, (a) at phi=0, when port2 is excited, (b) at phi=90, when port2 is excited, (c) at phi=0, when port3 is excited, (d) at phi=90, when port3 is excited, (e) at phi=0, when port1 is excited, (f) at phi=90, when port1 is excited.

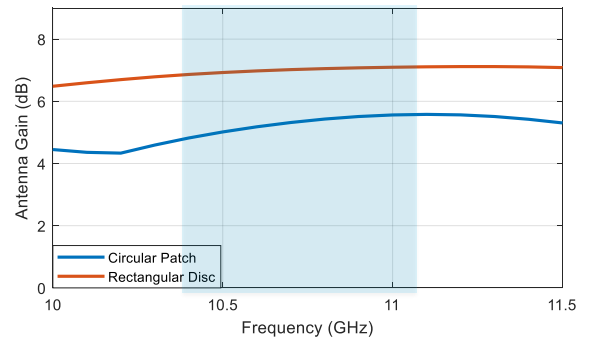


Fig.7 Gain versus frequency.

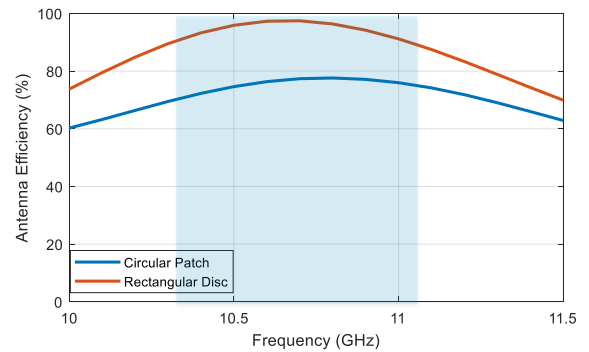


Fig.8 Efficiency versus frequency.

## 5 Conclusion

A dual-polarized microstrip antenna has been developed for X-band applications, operating at 10.6 GHz with a bandwidth of 600 MHz. The antenna incorporates two stacked substrates to support distinct geometries with varying radiation characteristics. The generation of a wide beamwidth radiation pattern is achieved by exciting the TM<sub>01</sub> mode through a short-circuited ring patch, producing a conical radiation pattern, along with the fundamental mode through a rectangular patch in the top layer. The implementation of dual-polarization is successfully realized. To validate the concept, the proposed design was fabricated and measured, demonstrating excellent agreement with simulated results. The antenna features a compact size, a broadside radiation pattern. The peak gains, illustrated over the frequency range, reach 5.2 dBi for the circular patch and 7 dBi for the rectangular patch. Additionally, radiation efficiency is highlighted, with rates of 89% and 98% at the central frequency for the circular and rectangular patches, respectively.

## References

- [1] Singh, Ajay Kumar, B. B. Padhy, and K. P. Ray. "Design of high-performance miniaturised circular slotted microstrip power dividers." *AEU-International Journal of Electronics and Communications* 174 (2024): 155013.
- [2] Liu, Gui, Peng Fei Hu, Guo Dong Su, and Yong Mei Pan. "Bandwidth and Gain Enhancement of a Single-Layer Filtering Patch Antenna Using Reshaped TM<sub>12</sub> Mode." *IEEE Antennas and Wireless Propagation Letters* (2023).
- [3] Abd El-Hameed, A. S., D. A. Salem, E. A. Abdallah, and E. A. Hashish. "Fractal quasi-self complimentary miniaturized UWB antenna." In *2013 IEEE Antennas and Propagation Society International Symposium (APSURSI)*, pp. 15-16. IEEE, 2013.
- [4] Abd El-Hameed, Anwer S., Deena A. Salem, Esmat A. Abdallah, and Essam A. Hashish. "Quasi self-complementary UWB notched microstrip antenna for USB application." *Progress In Electromagnetics Research B* 56 (2013): 185-201.
- [5] Abd El-Hameed, Anwer S., Haythem H. Abdullah, Deena A. Salem, and Esmat AF Abdallah. "Design of dual frequency notched semicircular slot antenna with semicircular tuning stub." *Progress In Electromagnetics Research* 599 (2012).
- [6] Fayyaz, Umar, Shahab Ahmad Niazi, Xingliang Zhang, Abdul Aziz, Khaled AlJaloud, and Rifaqat Hussain. "Effective Realization of Higher Order Circular Polarized OAM Mode Circular Patch Antenna." *IEEE Transactions on Circuits and Systems II: Express Briefs* (2023).
- [7] Flora J, Blessy Annie. "Rectangular Concentric Strip Antenna for IoT Applications." In *2023 International Conference on Sustainable Communication Networks and Application (ICSCNA)*, pp. 481-486. IEEE, 2023.
- [8] P. S. Hall, "Probe compensation in thick microstrip patches," *Electron. Lett.*, vol. 23, no. 11, pp. 606-607, 1987.
- [9] Q. Zhang, T. Yu, and J. Ye, "Microstrip monopolar patch antenna for bandwidth enhancement," *Progress In Electromagnetics Research Letters*, vol. 53, pp. 95-100, 2015.
- [10] Lin, Shun-Yun, and Kin-Lu Wong. "A stacked circular microstrip antenna for dual-band conical-pattern radiation." *Microwave and Optical Technology Letters* 28, no. 3 (2001): 202-204.
- [11] Ding, Xiaoxiang, Zhiqin Zhao, Yaohui Yang, Zaiping Nie, and Qing Huo Liu. "A low-profile and stacked patch antenna for pattern-reconfigurable applications." *IEEE transactions on antennas and propagation* 67, no. 7 (2019): 4830-4835.
- [12] Dahri, Muhammad Hashim, Mohd Haizal Jamaluddin, Mohsen Khalily, Muhammad Inam Abbasi, Raghuraman Selvaraju, and Muhammad Ramlee Kamarudin. "Polarization diversity and adaptive beamsteering for 5G reflectarrays: A review." *IEEE Access* 6 (2018): 19451-19464.
- [13] El-Nady, Shaza M., Anwer S. Abd El-Hameed, Eman M. Eldesouki, and Shimaa AM Soliman. "Circularly polarized MIMO filtering dielectric resonator antenna for 5G sub-6 GHz applications." *AEU-International Journal of Electronics and Communications* 171 (2023): 154882.
- [14] Elsharkawy, Rania R., Anwer S. Abd El-Hameed, and Shaza M. El-Nady. "Quad-port MIMO filter with high isolation employing BPF with high out-of-band rejection." *IEEE Access* 10 (2021): 3814-3824.
- [15] Sethi, Waleed Tariq, Mohammed R. AlShareef, M. Ashraf, Hatim M. Behairy, and S. Alshebeili. "Compact dual polarized aperture coupled microstrip patch antenna for UWB RFID applications." *Microwave and Optical technology letters* 59, no. 6 (2017): 1317-1321.
- [16] Guo, Yong-Xin, Michael Yan Wah Chia, Zhi Ning Chen, and Kwai-Man Luk. "Wide-band L-probe fed circular patch antenna for conical-pattern radiation." *IEEE Transactions on Antennas and Propagation* 52, no. 4 (2004): 1115-1116.
- [17] Feng, Botao, Jiexin Lai, Liangying Li, Li Deng, and Xiao Ding. "A Dual-Polarized Shared-Aperture Antenna With Conical Radiation Patterns and High Gain for 5G Millimeter-Wave Ceiling Communications." *IEEE Transactions on Antennas and Propagation* 71, no. 3 (2023): 2278-2289.
- [18] Pan YM., Leung KW. Wideband circularly polarized dielectric bird-net antenna with conical radiation pattern. *IEEE Trans Antennas Propag* (2013) 61(2):563-70. doi:10.1109/TAP.2012.2220101
- [19] Soliman, Ezzeldin A., Magdy S. Ibrahim, and Alaa K. Abdelmageed. "Dual-polarized omnidirectional planar slot antenna for WLAN applications." *IEEE transactions on Antennas and propagation* 53, no. 9 (2005): 3093-3097.

- [20] Hussain, Musa, Wahaj Abbas Awan, Mohammed S. Alzaidi, Niamat Hussain, Esraa Mousa Ali, and Francisco Falcone. "Metamaterials and their application in the performance enhancement of reconfigurable antennas: A review." *Micromachines* 14, no. 2 (2023): 349.
- [21] Nabar, Rohit U., Helmut Bolcskei, Vinko Erceg, David Gesbert, and Arogyaswami J. Paulraj. "Performance of multiantenna signaling techniques in the presence of polarization diversity." *IEEE Transactions on signal processing* 50, no. 10 (2002): 2553-2562.
- [22] Chen, Aixin, Weiwei Jiang, Zhizhang Chen, and Jiaheng Wang. "Overview on multipattern and multipolarization antennas for aerospace and terrestrial applications." *International Journal of Antennas and Propagation* 2013 (2013).
- [23] Lin, Wei, Hang Wong, and Richard W. Ziolkowski. "Wideband pattern-reconfigurable antenna with switchable broadside and conical beams." *IEEE Antennas and wireless propagation letters* 16 (2017): 2638-2641.
- [24] Zaghoul, Amir I., M. T. Kawser, and C. Babu Ravipati. "Modeling and analysis of a dual-Band dual-Polarization radiator using FEKO." *The Applied Computational Electromagnetics Society Journal (ACES)* (2007): 125-133.
- [25] V. González P., D. Segovia V., E. Rajo I., J. L. Vázquez R., and C. Martín P., "Analysis of Short Circuited Ring Patch Operated at TM<sub>01</sub> Mode," *Rev. Fac. Ing. - Univ. Tarapacá*, vol. 13, no. 2, 2005, pp. 21-30.
- [26] S. S. Qi, W. Wu, and D. G. Fang, "Dual/single band conical-beam nested horn antennas with dual/single pointing angles," *IEEE Trans. Antennas Propag.*, vol. 60, no. 10, pp. 4911-4915, Oct. 2012.
- [27] Cao, Yun Fei, Xiu Yin Zhang, and Te Mo. "Low-profile conical-pattern slot antenna with wideband performance using artificial magnetic conductors." *IEEE Transactions on Antennas and Propagation*, vol. 66, no. 5 (2018): 2210-2218.
- [28] J. H. Kim, and W. S. Park, "Sectoral conical beam former for a 2x2 array antenna," *IEEE Antennas Wireless Propag. Lett.* vol. 8, pp. 712-715, 2009.
- [29] Hany A. Atallah, Adel B. Abdel-Rahman, Kuniaki Yoshitomi, and Ramesh K. Pokharel, "Mutual coupling reduction between two-element array microstrip patch MIMO antenna using CSRRs DGS," *Applied Computational Electromagnetics Society Journal (ACES)*, vol. 31, no. 7, July 2016.
- [30] Hany A. Atallah, Adel B. Abdel-Rahman, Kuniaki Yoshitomi, and Ramesh K. Pokharel, "Design of miniaturized reconfigurable slot antenna using varactor diodes for cognitive radio systems," *2016 Fourth International Japan-Egypt Conference on Electronics, Communications and Computers (JEC-ECC)*, pp. 63-66, Egypt, 2016.
- [31] Hany A. Atallah, Adel B. Abdel-Rahman, Kuniaki Yoshitomi, and Ramesh K. Pokharel, "Tunable band-notched CPW-fed UWB monopole antenna using capacitively loaded microstrip resonator for cognitive radio applications," *Progress in Electromagnetic Research C (PIER C)*, vol. 62, pp. 109-117, January 2016.